EUROfusion

WPPFC-CPR(18) 18726

R Arredondo Parra et al.

Angle-dependent sputter-yield measurements of keV D ions on Fe and W with a new high-current ion source

Preprint of Paper to be submitted for publication in Proceeding of
23rd International Conference on Plasma Surface Interactions in
Controlled Fusion Devices (PSI-23)

This work has been carried out within the framework of the EUROfusion Consortium and has received funding from the Euratom research and training programme 2014-2018 under grant agreement No 633053. The views and opinions expressed herein do not necessarily reflect those of the European Commission.

Angle-dependent sputter yield measurements of keV D ions on W and Fe and comparison with SDTrimSP and SDTrimSP-3D

R. Arredondo[1,2,*], M. Oberkofler[1], T. Schwarz-Selinger[1], U. von Toussaint[1], V. V. Burwitz[1,2], A. Mutzke[3], E. Vassallo[4], M. Pedroni[4]

July 24, 2018

[1] *Max-Planck-Institut für Plasmaphysik, Boltzmannstr. 2, D-85748 Garching, Germany*

[2] *Technische Universität München, Boltzmannstr. 15, D-85748 Garching, Germany*

[3] *Max-Planck-Institut für Plasmaphysik, Wendelsteinstrasse 1, D-17491 Greifswald, Germany*

[4] *CNR-Istituto di Fisica del Plasma, via R. Cozzi 53, 20125 Milano, Italy*

[*] *rodrigo.arredondo@ipp.mpg.de*

Abstract

The sputter yield of first-wall materials upon bombardment with energetic particles stemming from a fusion plasma is a relevant parameter for the operational lifetime of a future fusion power plant. As part of ongoing research on the influence of surface roughness on the sputter yield, nm-smooth and rough samples with roughnesses on the µm length scale were produced by depositing thin Fe and W films on smooth and rough Si substrates via magnetron sputtering. The surface morphology of the samples was determined by atomic force microscopy. The samples were exposed at SIESTA (Second Ion Experiment for Sputtering and TDS Analysis) to a 6 keV D_3^+ ion beam (2 keV/D) under various angles of incidence ranging from 0° to 75° with respect to the surface normal to fluences of the order of $10^{22}\,\mathrm{D/m^2}$. The layer thickness was measured by Rutherford backscattering spectrometry (RBS) before and after erosion. The resulting sputter yields were compared to simulations performed with SDTrimSP (static and dynamic) and SDTrimSP-3D (static), showing good qualitative agreement in all cases, as well as agreement with literature data at normal incidence. This constitutes the first experimental benchmark of SDTrimSP-3D. A discrepancy in the value of the sputter yield for smooth W at normal incidence was observed between the SDTrimSP simulations and the experimental values obtained in this work and found in literature. Analogous experiments were performed to study the sputter yield at normal incidence of 2 keV/D on smooth Au and 6 keV He on smooth W. These sputter yields were also compared to SDTrimSP simulations and literature, showing good agreement in all cases.

1 Introduction

Physical sputtering by energetic particle bombardment is the main physical process driving erosion of plasma-facing materials in a nuclear fusion device [1]. Physical sputtering also plays an important role in other plasma-surface interaction processes such as magnetron sputtering, ion milling or analysis methods such as sputter-XPS or SIMS, and it has been the focus of extensive experimental and theoretical research in the past. Monte Carlo codes simulating sputtering by Coulomb interactions have been developed (e.g., SDTrimSP [2]), providing good agreement with experimental values for a wide range of ion-target combinations [3]. This process can be studied experimentally, either in plasma devices or with the use of an ion source. Ion sources have a number of distinct advantages over plasma devices, as they enable the extraction of a mono-energetic beam which can be mass-filtered with magnetic sector fields. The ensuing knowledge of the impinging particle species and energy can be coupled with accurate ion current measurement techniques to allow for well-defined experiments.

As noted in e.g. [4] and [5], target surface roughness can have a significant impact on the net sputtering behavior of a material under bombardment. Depending on the specific surface morphology and nominal angle of incidence (i.e., the angle of incidence measured relative to the global surface normal), increased or decreased sputtering with regards to a perfectly smooth surface may occur, based on a superposition of two effects. On the one hand, due to surface roughness, the local incident angle will differ from the nominal incidence, as the nominal incident angle will be offset by the local slope at each point on the surface. This variation typically leads to increased sputtering when the nominal incidence is close to normal [6]. On the other hand, on rough surfaces re-deposition may play a role, as a particle sputtered from one point on the surface has a chance of impinging on another point on the surface and re-depositing, thereby reducing global net erosion. Within this work, as part of ongoing research into the influence of surface roughness on sputtering, the previously unmeasured angle-dependent sputter yields for D bombardment of W and Fe were determined. This was achieved by exposing smooth W and Fe thin films to a 6 keV D_3^+ (2 keV/D) ion beam at the newly-built high-current ion source SIESTA (Second Ion Experiment for Sputtering and TDS Analysis) [7] and measuring the ensuing eroded layer thickness by Rutherford backscattering spectrometry (RBS) with a 2 MeV He^+ ion beam. The sputter yield data are compared with SDTrimSP simulations (assuming perfectly smooth samples) and experimental data from literature at normal incidence. Additionally, the angle-dependent sputter yield of rough W samples was measured and compared with static SDTrimSP-3D [8] simulations based on the sample surface morphology extracted from atomic force microscopy (AFM) scans, constituting the first experimental benchmark of the 3D-version of the code. Results are presented and discussed in section 3. Section 4 constitutes a summary of these results.

2 Experimental procedure and simulations

As mentioned in sec. 1, part of the goal of this work was the comparison of sputter yields for smooth and rough samples. For this purpose, it was decided that the surface morphology of the samples to be studied should be modified as little as possible by the impinging ion beam. To comply with this restriction, it was decided to expose the samples to low fluences, of the order of 10^{22} D/m^2, corresponding to eroded layer depths of the order of tens of nm. This motivated the use of RBS to measure the thickness of nm-thin films, as the film thickness averaged over the analysis beam-spot (approx. 1x1 mm in our case) could be measured before and after implantation with sub-nm accuracy.

In [8] the effect of roughness on the sputter yield was evaluated on a synthetic sinusoidal cone surface. It was shown that at an aspect ratio of one, corresponding to a maximum incident angle of 45° and R_{RMS} (Root Mean Square Roughness) value of approximately 7 nm, surface roughness plays a significant role on the sputter yield, as it is reduced by around 30%. Based on these findings, in this work, the maximum incident angle is used as a criterion to define whether a surface is smooth or rough. A surface is considered smooth if the maximum incident angle measured by AFM is much lower than 45°. To reduce the influence in this evaluation of potential outliers in the AFM measurement, the value of the incident angle at the 95th percentile of the slope distribution was used to judge whether the surface was considered rough or smooth.

500 nm-thick Fe films were deposited by magnetron sputtering on smooth Si samples of 12 × 15 mm^2 surface area. As deposited, the samples exhibited a corrugated surface morphology in the nm-scale (fig. 1) and an angle of incidence at the 95th percentile of the slope distribution of 48°. The samples were, therefore, considered rough. To reduce the surface roughness of the films, they were eroded for 3 hours to a thickness of 260 nm by an Ar plasma at a pressure of 1 Pa under a bias voltage of 200 V in the magnetron sputtering device. AFM was performed with an Asylum Research MFP-3D[1] device to characterize the surface morphology of the samples before and after erosion with Ar (fig. 1). The morphology changed from a corrugated structure with R_{RMS} values of 13 nm to smooth hills and valleys of $R_{RMS} < 4$ nm. The slope distribution of the smoothed samples is such that 95% of all measured points on the sample are on areas with an inclination lower than 15°. Typical local slope distributions are shown in figure 2. As expected, progressive smoothing increases the preponderance of flat angles, confirming that after erosion with Ar the sample is smooth. The smooth W samples were produced by magnetron sputtering a 60 nm thick Cr interlayer on smooth 12×15 mm^2 Si samples and depositing a 60 nm-thick W layer on top of the Cr layer. The Cr interlayer served to improve adhesion of the W layer. AFM scans showed that the as-deposited samples were sufficiently smooth (fig. 4), with $R_{RMS} \simeq 0.5$ nm and a distribution of inclination angles lower than 7° for 95% of the measured points on the sample (fig. 2). The rough W samples were produced by depositing a 100 nm-thick W layer on a 150 nm-thick Ti interlayer on a nanostructured Si substrate via magnetron sputtering. The Ti interlayer served the same purpose as the Cr interlayer for the smooth samples. The nanostructured silicon was prepared by means of a mask-less plasma process employing tetrafluoromethane and hydrogen as reaction gases. Surface texturing was achieved by an overall etching process with a simultaneous random deposition of a passivation layer produced by H particles, CFx radicals and the partially etched product SiFx. The competition between passivation layer deposition and its removal by bombardment with energetic ions causes local variations of the etching rate on the Si surface, leading to the growth of random silicon nanostructures over the process time [9]. A scanning electron microscopy cross section of a rough W sample, produced by focused ion beam milling, is shown in figure 3. AFM scans of these samples indicated a $R_{RMS} \simeq 20$ nm and a distribution of local slopes lower than 50° for 95% of all measured points (figs. 4, 2). The roughness values of these samples and their slopes at the 95th percentile are listed in table 1.

The samples were exposed under incident angles of 0° (normal incidence), 45°, 60° and 75° to a 6 keV D_3^+ beam (2 keV/D) at SIESTA [7]. The surface area of the beam footprint at the target was measured in all cases by eroding 70 nm-thick amorphous hydrogenated

[1] Trademark of Oxford Instruments Asylum Research, Inc.

Sample	R_{RMS} [nm]	Slope dist. (95%)
Fe rough	13.4	48°
Fe smooth	3.7	15°
W rough	19.6	50°
W smooth	0.6	7°

Table 1: Root mean squared roughness values of Fe and W samples and the slope at the 95th percentile.

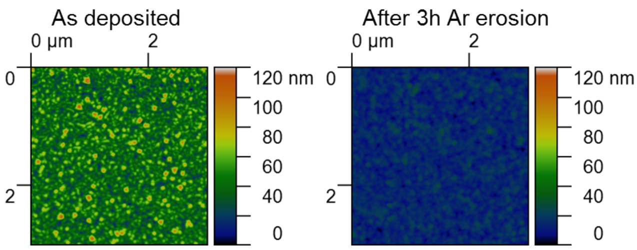

Figure 1: Atomic Force Microscopy images of 500 nm magnetron-deposited Fe thin films on Si, before (left) and after 3 hours of erosion under an Ar plasma (right). The samples are smoothed by the Ar plasma to $R_{RMS} < 4\,\mathrm{nm}$, as listed in tab. 1. (Color online).

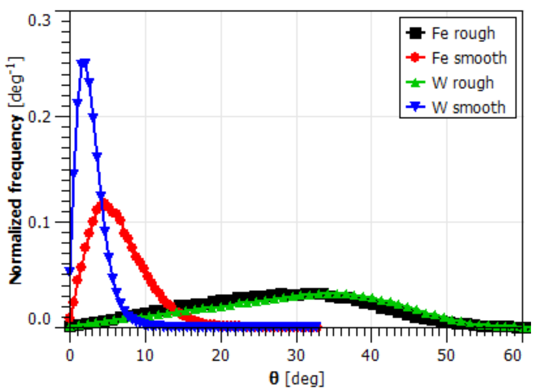

Figure 2: Typical distributions of local slopes of rough and smooth Fe and W thin films deposited on Si by magnetron sputtering. The local slope corresponding to the 95th percentile is listed in tab. 1. (Color online).

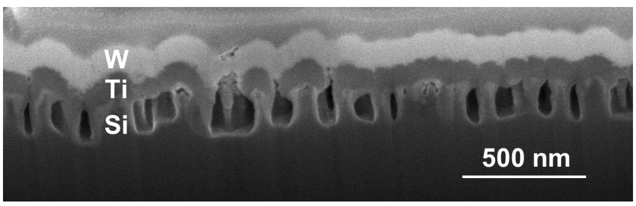

Figure 3: Scanning electron microscopy cross section of a rough W sample, produced by focused ion beam cut. The W and Ti thin films and roughened Si substrate have been labeled in white.

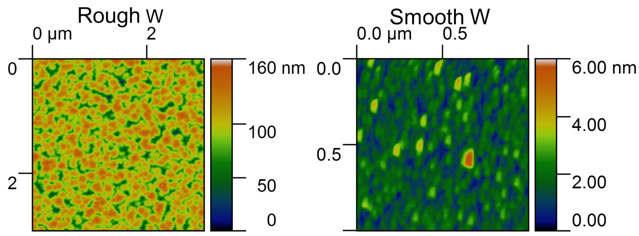

Figure 4: AFM images of rough (left, 3x3 µm) and smooth (right, 1x1 µm) W samples. The height scale of the smooth W image has been reduced to improve the visibility of the surface roughness. TheR_{RMS} values of the samples are listed in tab. 1. (Color online).

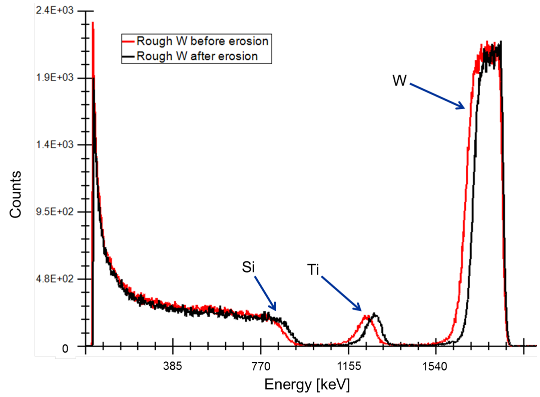

Figure 5: RBS spectra of a rough W sample before (red) and after exposure at SIESTA (black) under 0° incidence. The integral of the W peak is proportional to the thickness of the W layer. The width of the W peak after exposure has diminished due to erosion. (Color online).

carbon layers (a-C:H) on a Si substrate under identical exposure conditions. The measured surface area was used to estimate the ion fluence to the targets. The samples were eroded to fluences in the range of $10^{22}\,\mathrm{D/m^2}$, equating to an erosion of $\sim 10\,\mathrm{nm}$. Before and after erosion, the samples were analyzed by RBS at the Tandem accelerator at IPP, using 2 MeV He ions and a scattering angle of 165°. Figure 5 shows typical spectra from a rough W sample analyzed before and after erosion at SIESTA. The integral of the W signal is proportional to the areal density of the W surface layer. The layer thickness can be deduced from the measured areal density by dividing by the atomic density of the W layer, which as a first approximation can be assumed to be the atomic density of bulk W.

From the data, the sputter yield for each angle of incidence was calculated by applying the equation:

$$Sputter\,Yield = \frac{N_{eroded}\,[\mathrm{at/cm^2}] * S\,[\mathrm{cm^2}]}{N_{impinging}\,[\mathrm{at}]}, \qquad (1)$$

where N_{eroded} denotes the thickness of the eroded layer in atoms per unit surface, S is the surface area of the beam-spot at the target and $N_{impinging} = 3 * Q/e$ is the total amount of impinging deuterons. Q is the collected charge at the target and e is the elementary charge. These results were compared with lit-

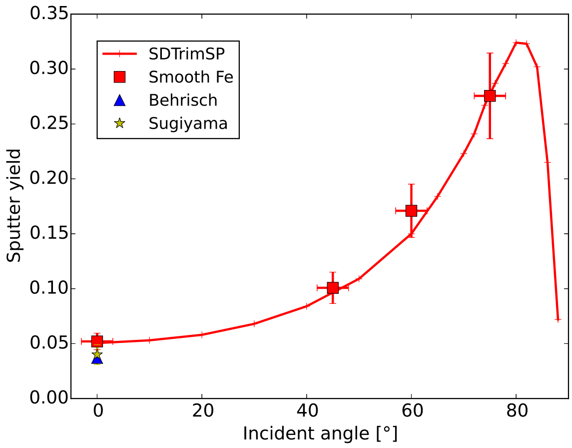

Figure 6: Sputter yields of a 6 keV D_3^+ beam (2 keV/D) on smooth Fe thin films under incident angles of 0° (normal to surface), 45°, 60° and 75°, determined by RBS. SDTrimSP simulations and literature values from Behrisch and Eckstein [10] and Sugiyama [11] are included for comparison. (Color online).

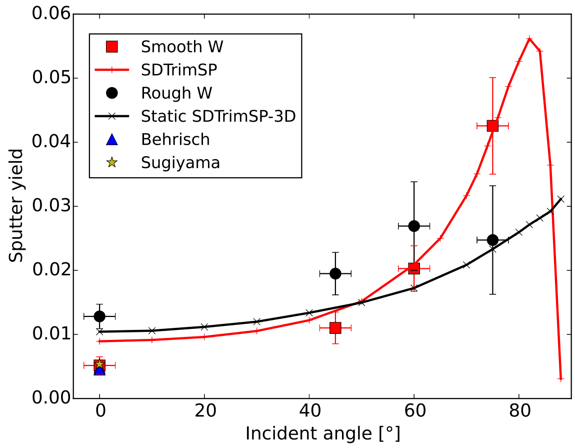

Figure 7: Sputter yields of a 6 keV D_3^+ beam (2 keV/D) on smooth (red squares) and rough (black circles) W thin films under incident angles of 0° (normal to surface), 45°, 60° and 75°. The smooth W data can be directly compared to 1D SDTrimSP simulations (red curve with + symbols), while the rough W data may be compared with static SDTrimSP-3D simulations (black curve with crosses). Literature values from Behrisch and Eckstein [10] and Sugiyama [11] are included for comparison. (Color online).

erature data and with the sputter yields calculated with SDTrimSP for the given experimental conditions. SDTrimSP is a monte-carlo code which simulates transport of energetic particles through a target by employing the two-body collision approximation. In the 1D version, the target consists of laterally homogeneous layers of arbitrary composition. Said simulations were performed with the standard parameters (Gauss-Mehler quadrature integration method with 8 pivots and ipot set to 1) [2]. For the static simulations of erosion of the rough W samples with SDTrimSP-3D [8], the surface geometry was directly extracted from the AFM scans of the samples (fig. 4), consisting of a simulated surface of 440.25 x 440.25 nm. This is considered a representative area of the overall surface morphology. The cell resolution for the 3D simulation was $5.87 \times 5.87\,\mathrm{nm}^2$.

The experimental uncertainties of the measured sputter yields were calculated. The measurement uncertainty depends on the variance of N_{eroded} (number of counts of the integral of the RBS spectrum), S (beam footprint at the target) and Q (accumulated charge). In practice, the uncertainty due to N_{eroded} is negligible due to sufficient statistics in the RBS spectra. The uncertainty in S is in the range of $\pm 0.05\,\mathrm{cm}^2$ (approx. 7% of surface area) at low angles of incidence (impinging ion beam footprint is well defined and homogeneous), but it is significant at high angles of incidence, up to $\pm 0.3\,\mathrm{cm}^2$, corresponding to 30% of surface area, for samples eroded under 75° incidence. The uncertainty in Q is linked to the relative error of the ion current measurement, which was estimated to be 14% [7].

3 Results and discussion

The experimental and simulated results for the smooth Fe thin films are shown in fig. 6. The experimental results agree fully with the simulated values within the experimental uncertainty. The sputter yield increases with the angle of incidence. In the simulation, the SY reaches a maximum for an angle of about 80° and then sharply decreases due to increased reflection. The experimentally determined sputter yield under normal incidence is approximately 20% larger than the values given in the literature [10, 11], though they agree within the experimental uncertainty in the case of [11]. No estimation of uncertainty is given in [10].

The results from the smooth and rough W thin films are shown in fig. 7. The experimentally determined sputter yield of the smooth W sample under 0° incidence displays a discrepancy of a factor of 2 with SDTrimSP. However, there is good agreement with the literature data for smooth W at normal incidence from [10, 11], indicating that this discrepancy may be an issue with SDTrimSP and not with the experiment. All other data points of the smooth W sputter yields are in agreement with the SDTrimSP calculations. Both experimental and simulated curves show a similar trend to what is observed with smooth Fe. Contrary to the sputtering behavior of the synthetic surfaces in [8], the static SDTrimSP-3D calculations indicate an increase in the SY at normal incidence. The reason for this different behavior is likely the very different slope distributions of the rough W samples and the synthetic surface, when the latter is evaluated at roughness values comparable to those measured on the rough W samples. The simulations agree qualitatively with the sputter yields of the rough W thin films. As was the case with the smooth samples, the sputter yield of the rough samples increases as a function of the nominal incident angle within the measured range of 0° to 75°, though this increase is less pronounced than for the smooth samples and no sputter yield maximum is observed. SDTrimSP-3D correctly predicts increased sputtering of the rough surfaces at low angles of incidence ($< 50°$) and decreased sputtering at high angles of incidence ($> 60°$) as compared to the smooth surfaces. However, SDTrimSP-3D deviates significantly from the measurements at 45° and 60° incidence, which could be in part a consequence of the limited resolution of the AFM scans when imaging sharp changes in the slope of the surface, as the scan is "smoothed" over the scanning tip radius of 10 nm.

Overall, the results for the smooth and rough W thin films present a similar trend to those observed by Küstner et al. in [4] and [5], where respectively the sputter yields of 2 keV D^+ on pyrolytic and isotropic graphite, and of 3 keV Be^+ on polished, roughened and unpolised Be were measured as a function of the angle of incidence and compared to SDTrimSP .

The mismatch of a factor of 2 between SDTrimSP and the smooth W sample at 0° incidence is not observed between SDTrimSP-3D and the rough W sample. A static SDTrimSP-3D simulation was performed with the surface morphology of the smooth W samples. The resulting sputter yields correctly reproduced the SDTrimSP results, presenting the same mismatch at 0° incidence. In order to assess whether this discrepancy is related to the chosen projectile or target, the sputter yields of 6 keV D_3^+ (2 keV/D) on Au and 6 keV He^+ on W were measured under normal incidence and compared to data from SDTrimSP simulations and literature [10, 12]. The measurements on Au have been previously described in [7]. All data are listed in tab. 2. As was the case with Fe, the experimental sputter yield of D on Au agrees reasonably well with SDTrimSP (experimental sputter yield is 12% larger), and is slightly higher than other values from literature. The experimental sputter yield of He on W shows very good agreement with the data from literature, but is approximately 35% smaller than the value given by SDTrimSP. While this mismatch is significant, it is substantially smaller than the factor of 2 discrepancy between experiments and simulation for D on smooth W. Similar discrepancies between experimental SY and sputter yields calculated with SDTrimSP were also observed in literature data for W and other brittle materials (e.g., Mo, B, Be), both in magnitude and direction ($SY_{simulated} > SY_{experimental}$), regardless of impinging ion species, while the agreement is better for more ductile materials (Cu, Ni, Au) [10]. It is possible that the binary collision approximation, on which SDTrimSP is based, is less applicable for brittle materials than for ductile ones. However, this conjecture alone would fail to explain why said discrepancy is not observed in the case of rough W at normal incidence or smooth W at higher angles. One explanation for this lack of discrepancy could be that W exhibits grain-orientation-dependent sputtering and the predominant grain orientation, i.e., the texture of the two sets of samples, may be different. Recent experiments with W have indicated a strong (factor of 10) dependence of the sputter yield on the W grain orientation [13], and since the surface morphologies of the substrates on which the smooth and rough W thin films were deposited were different, it is conceivable that the two sets of samples exhibited preferential layer growth in different crystallographic orientations.

4 Summary

A series of smooth Fe and W and rough W thin films were eroded by ion bombardment with a 6 keV D_3^+ (2 keV/D) ion beam under well-defined laboratory conditions at SIESTA. The sputter yield under these conditions was measured as a function of the angle of incidence by determining the eroded layer thickness with 2 MeV He^+ RBS measurements performed before and after erosion. The surface morphology of the thin films was characterized with AFM before erosion. The ensuing sputter yield values are compared with SDTrimSP simulations, literature data at 0° incidence and, in the case of the rough thin films, static SDTrimSP-3D simulations based on the sample surface morphology from the AFM scans. This constitutes the first experimental benchmark of SDTrimSP-3D.

The sputter yield data from the smooth Fe thin films showed quantitative agreement with the SDTrimSP simulations in all cases. The sputter yields from the smooth W thin films agreed quantitatively with the SDTrimSP simulations in all cases except under normal incidence, where a discrepancy of a factor of two was observed. Since the experimentally-determined sputter yield under normal incidence agrees with the data from literature, it was concluded that this mismatch was due to an issue with SDTrimSP and not with the experiment. Reasons for this mismatch were proposed, consisting of a systematic error by SDTrimSP when calculating the sputter yield of brittle targets, as indicated by a review of the existing literature [10]. Another factor could be the effect of the grain orientation of the W films on the measured sputter yields, as recent investigations have shown that W may exhibit grain-orientation-dependent sputtering under certain exposure conditions [13]. This last point is currently the focus of ongoing investigations.

There is qualitative agreement between the sputter yields of the rough W thin films and the SDTrimSP-3D calculations. In this experimental benchmark, the code correctly predicted an increase of the sputter yield with the angle of incidence, increased sputtering of the rough surface relative to the smooth case at low angles of incidence and decreased sputtering compared with the smooth case at high angles of incidence. The aforementioned discrepancy in the sputter yield at normal incidence was not observed when comparing the rough samples with SDTrimSP-3D simulations.

The sputter yield trends observed in the experiments and simulations can be explained qualitatively. If the local incident angle of the projectile on the surface is high, a large fraction of the projectile energy is deposited closer to the surface. This increases the proba-

Sputter yields	2 keV/D on Fe	2 keV/D on W	2 keV/D on Au	6 keV He on W
Experimental	0.0459 ± 0.0075	0.0052 ± 0.0014	0.0419 ± 0.002	0.0474 ± 0.0099
SDTrimSP	0.051	0.0128	0.037	0.063
Behrisch [10]	0.040	0.0048	0.031	0.045
Sugiyama [11]	0.040 ± 0.009	0.0054 ± 0.001		
Bay [12]			0.038	

Table 2: Sputter yields under normal incidence of 6 keV D_3^+ (2 keV/D) on smooth Fe and on smooth W and Au, and of 6 keV He^+ on W, determined experimentally (with uncertainty), via SDTrimSP simulations, or from literature (with uncertainty where available). The experimental data for D on Au was determined by mass-loss measurements and was previously presented in [7].

bility for a surface atom to receive enough energy to be sputtered. However, at very high angles (close to grazing incidence), decreased sputtering is observed. In the case of rough surfaces, when the angle of incidence is close to the surface normal, the local incident angles (slopes) are higher than the nominal angle of incidence, contributing to an increase in the local sputter yield. When the angle of incidence is high, there are contributions from both sides of the sputtering maximum: parts of the surface may exhibit increased sputtering due to high local slopes, while others may exhibit decreased sputtering due to low local slopes or grazing incidence. Additionally, in the case of rough samples there is a probability of re-deposition of a sputtered atom, contributing to lower net sputtering. However, in the case of the morphology of the rough W samples examined in this work, the effect of re-deposition seems to be less important than the effect of the angles of incidence.

Acknowledgements

The authors would like to express their gratitude to K. Sugiyama, H. Gietl, S. Elgeti, T. Höschen, A. Friedrich, A. Weghorn, M. Fußeder, J. Dorner and the E2M workshop for their continued support.

This work has been carried out within the framework of the EUROfusion Consortium and has received funding from the Euratom research and training programme 2014-2018 under grant agreement No 633053. The views and opinions expressed herein do not necessarily reflect those of the European Commission. Work performed under EUROfusion WP PFC.

References

[1] J. Roth et al. Recent analysis of key plasma wall interactions issues for ITER. *J. Nucl. Mater.*, 390-391:1–9, 2009.

[2] A. Mutzke, R. Schneider, W. Eckstein, and R. Dohmen. *SDTrimSP Version 5.00.* IPP Report 12/08, Max-Planck-Institut für Plasmaphysik (Ed.) http://hdl.handle.net/11858/00-001M-0000-0026-EAF9-A, 2011.

[3] W. Eckstein. *Computer Simulation of Ion-Solid Interactions.* Springer Berlin Heidelberg, 1991.

[4] M. Küstner, W. Eckstein, V. Dose, and J. Roth. The influence of surface roughness on the angular dependence of the sputter yield. *Nucl. Instrum. Methods Phys. Res., Sect. B*, 145(3):320–331, nov 1998.

[5] M Küstner, W Eckstein, E Hechtl, and J Roth. Angular dependence of the sputtering yield of rough beryllium surfaces. *J. Nucl. Mater.*, 265(1):22 – 27, 1999.

[6] R. Behrisch and W. Eckstein. Introduction and overview. In *Sputtering by Particle Bombardment*, chapter 1. Springer Berlin Heidelberg, 2007.

[7] R. Arredondo, M. Oberkofler, K. Schmid, T. Schwarz-Selinger, W. Jacob, and R. Neu. SIESTA: a high current ion source for erosion and retention studies. *Rev. Sci. Instrum.*, Submitted, awaiting publication, 2018.

[8] U. von Toussaint, A. Mutzke, and A. Manhard. Sputtering of rough surfaces: a 3D simulation study. *Phys. Scr.*, 2017(T170):014056, 2017.

[9] E. Vassallo et al. Black-silicon production process by CF4/H2 plasma. *Thin Solid Films*, 603:173 – 179, 2016.

[10] W. Eckstein. Sputtering yields. In R. Behrisch and W. Eckstein, editors, *Sputtering by Particle Bombardment IV*, volume 110 of *Topics in Applied Physics*, chapter Sputtering Yields, pages 33–187. Springer Berlin Heidelberg, Berlin, 2007.

[11] K. Sugiyama, K. Schmid, and W. Jacob. Sputtering of iron, chromium and tungsten by energetic deuterium ion bombardment. *Nucl. Mater. Energy*, 8:1–7, 2016.

[12] H. L. Bay, J. Roth, and J. Bohdansky. Light-ion sputtering yields for molybdenum and gold at low energies. *J. Appl. Phys.*, 48(11):4722–4728, 1977.

[13] K. Schlüter. Personal communication. 2018.